Scaling Synthesis of Sulfur Cathode Materials: an Analysis of Sulfur Distribution to Achieve High Performing Lithium-Sulfur Batteries

Wilson Shi Jie Ng

A thesis

submitted in partial fulfillment of the

requirements for the degree of

Master of Science

University of Washington

2025

Committee:

Jie Xiao

Jun Liu

Program Authorized to Offer Degree:

Materials Science & Engineering

University of Washington

Abstract

Scaling Synthesis of Sulfur Cathode Materials: an Analysis of Sulfur Distribution to Achieve High Performing Lithium-Sulfur Batteries

Wilson Shi Jie Ng

Chair of the Supervisory Committee:

Jie Xiao

Department of Mechanical Engineering

As a promising candidate for next-generation high performance lithium batteries, lithium-sulfur (Li-S) technology has been widely explored in academia. With a wide variety of cathode materials validated, the next step towards practical development is to be able to scale up their production while maintaining consistent quality. This thesis focuses on the lab-scale synthesis of a nitrogen-doped Ketjen Black/sulfur (NKB/S) composite material with the goal of producing batches at a consistent quality and identifying any scientific problems along the way that could hold implications for future scale-up work. During material and electrochemical validation, it was found that the sulfur content distribution consistently deviated from the target set during synthesis across particle sizes. Sulfur distribution in the usable 25-90µm NKB/S was found to consistently have 2-4% extra wt.% sulfur than the target, while the material <25µm were missing almost an equivalent amount of sulfur. Theories behind this phenomenon and further validations are discussed and proposed.

1. Introduction

1.1 Introduction to Lithium-Sulfur Batteries

Lithium-sulfur (Li-S) batteries present a promising alternative to the mature lithium-ion battery chemistries that dominate the consumer market. Possessing both a high theoretical energy density (~2500Wh/kg) and specific capacity (1675mAh/g) combined with its low cost and environmental friendliness, sulfur (S) has long been regarded as a good candidate for next-generation lithium (Li) batteries [1-2]. However, this chemistry suffers from several challenges that prevent wider use and commercialization: the poor electronic and ionic conductivities of S and lithium sulfide (Li_2S), the polysulfide shuttling effect, large volume changes when lithiating and delithiating, and the challenge of achieving high mass loading in the cathode while maintaining good cell operation [1-2]. This section offers a brief introduction to Li-S batteries and cathode materials in order to provide insight into some of the fundamental issues surrounding this battery type and where the scope of this project fits into the larger goal of manufacturing high-performance Li-S cathode materials.

1.1.1 Li-S Chemistry and the Polysulfide Shuttle Effect

Li-S cells use sulfur, or a sulfur-containing material, as a cathode with Li metal as the anode. Despite a lower average operating voltage of 2.1V, the large theoretical capacities for the two materials (S 1675mAh/g, Li 3680mAh/g) give the system a large theoretical energy density (~2500Wh/kg) [2]. A typical voltage profile is shown in **Figure 1**. This chemistry operates according to the chemical reaction shown in Equation 1 [2]:

$$S_8 + 16Li \rightleftharpoons 8Li_2S \quad (1)$$

The distinct double-plateau shape of the Li-S voltage profile indicates the presence of several intermediate reactions, whereby lithium polysulfides of the form Li_2S_x (x = 2, 4, 6, 8) are formed.

In the first plateau, sulfur, most naturally occurring in the form of S_8, reduces to Li_2S_8 (Equation 2) before reducing down to Li_2S_6 and Li_2S_4 (Equation 3) [3]:

$$S_8 + 2Li \rightleftharpoons Li_2S_8 \quad (2)$$

$$Li_2S_8 + 2Li \rightleftharpoons Li_2S_{8-x} + Li_2S_x \quad (3)$$

At the second plateau, Li_2S_4 mainly reduces towards the last drop-off, where the formation of Li_2S_2 (Equation 4) and Li_2S (Equation 5) completes the reaction [3]:

$$2Li_2S_x + (2x-4)Li \rightarrow xLi_2S_2 \quad (4)$$

$$Li_2S_x + (2x-2)Li \rightarrow xLi_2S \quad (5)$$

The intermediate polysulfides (Li_2S_8 - Li_2S_4) are very soluble in conventional ether-based electrolytes, which improves sulfur utilization [3-4]. This term refers to how closely the system can get to achieving the full theoretical capacity of sulfur – the higher the sulfur utilization, the higher the specific capacity the system will achieve. However, this high solubility leads to a phenomenon known as polysulfide shuttling. Dissolved polysulfides can diffuse out of the cathode along concentration gradients, across the separator membrane and come into contact with the Li metal anode [3, 5]. While doing so, they can also undergo uncontrolled parasitic side reactions with the Li metal anode, depositing insoluble Li_2S_2/Li_2S onto the anode surface [3]. This leads to rapid and severe sulfur material loss [3, 5]. Coupled with the electrolyte degradation caused by continuous polysulfide diffusion through the electrolyte, these all contribute towards shortening the cell's cycle life [3, 5]. It has been found, however, that certain electrolyte additives (such as lithium nitrate) have been able to aid in suppressing this shuttling effect to better promote the main electrochemical reaction [4, 5].

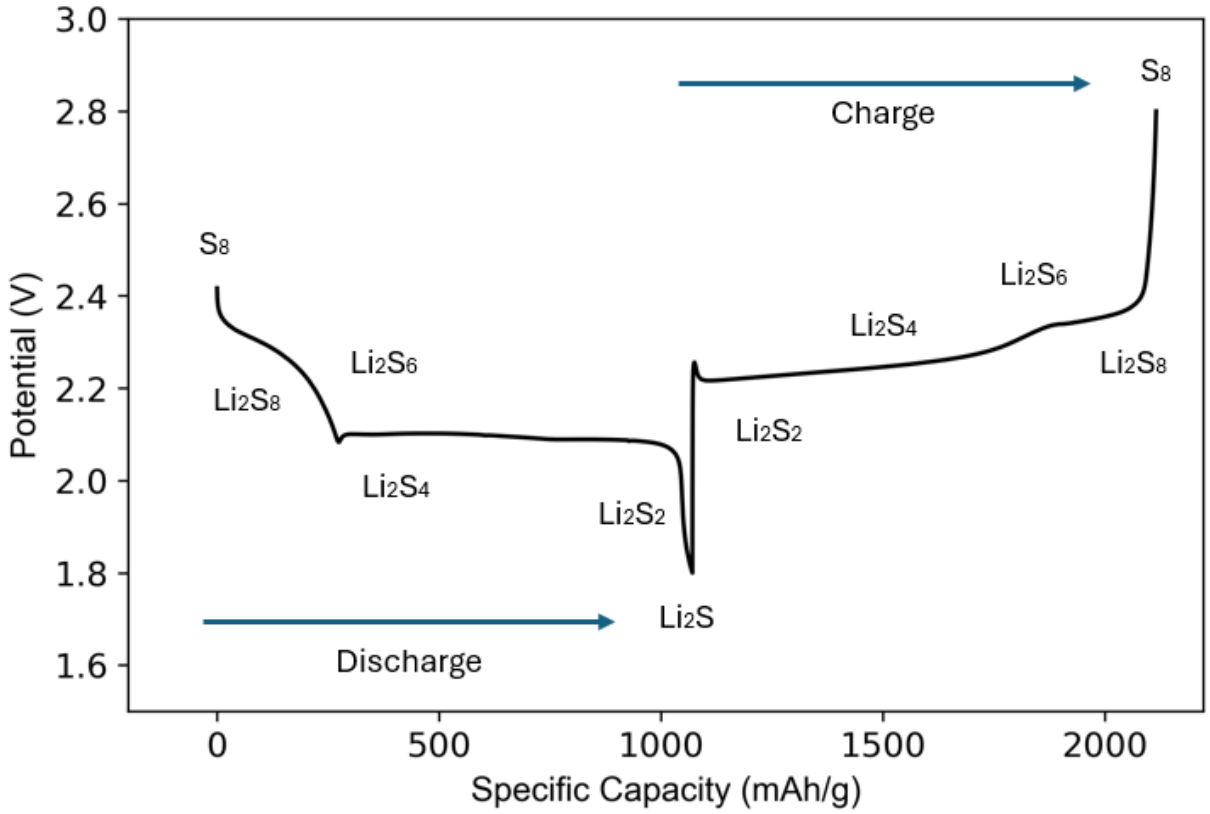

Figure 1. Typical charge/discharge voltage profile of a Li-S battery

1.1.2 Li-S Cathode Materials

In order to take advantage of this chemistry, a large variety of materials have been proposed as the sulfur cathode. Some cathodes utilize Li sulfide composite materials, essentially undergoing the Li-S electrochemical reaction in reverse [6]. Others might chemically bind the sulfur to a polymer, such as in the case of sulfurized polyacrylonitrile (SPAN) [7]. Many of the most researched materials for this battery chemistry, however, are elemental sulfur composites with conductive hosts [6]. These hosts physically integrate elemental sulfur within their porous frameworks to facilitate the electrochemical reactions that power the battery.

One of the most common types of sulfur composites in literature are sulfur-carbon (S/C) composites. These materials involve conductive carbon hosts with elemental S infused into them.

Almost every different type of porous, hollow or structured carbon material has been explored in literature in some way. These include amorphous carbon black, carbon spheres, carbon nanomaterials (such as nanofibers and nanotubes), graphene/graphene oxide, etc. [3, 8]. On top of having the advantage of being inherently electronically conductive, these carbons also offer the ability for the cathode to better trap polysulfide species and provide sites for the sulfur electrochemical reactions to occur [3]. Another type of host material that has been proposed are conductive polymers, such as polythiophene (PT), polyaniline (PANI) and polypyrrole (PPY) [2, 9-11]. These composites are typically synthesized by oxidative polymerization of the monomer onto sulfur particles to encase them [2]. Being naturally more elastic, sulfur-polymer composites are able to better maintain structure while the cathode undergoes volumetric changes during cycling [2].

This work focuses on a S/C composite material and how to further develop this technology for practical application. Namely, achieving the following [1]:

1) Have a feasible and scalable synthesis process, preferably at as low of a cost as possible
2) Support a high sulfur content, high sulfur loading and a high sulfur utilization rate
3) Operate well under practical conditions (low electrolyte-to-sulfur ratio, low cathode porosity)

1.2 NKB/S

Within the realm of S/C composites, a key strategy towards enhancing cell performance on the cathode side is to dope the carbon host with nitrogen (N). This enhances the cathode's ability to trap polysulfides, preventing active material loss and allowing the cell to maintain a high sulfur utilization through the interaction between N and S [12]. In the synthesis process, Ketjen Black

nanoparticles form an N-doped secondary particle in a two-step process that produces a carbon host structure that can confine sulfur and polysulfides [1]. The broader goal of this study is to identify scientific problems that are potentially associated with scaling up the synthesis process of this material. **Table 1** outlines the general three-step process towards synthesizing this N-doped Ketjen Black-sulfur (NKB/S) composite and quality control considerations along each step that could be considered when planning equipment and process updates or adjustments for scaling up synthesis. The following work explores the uneven sulfur content and distribution across batches of NKB/S with the goal of achieving consistent quality batches at a lab scale, while identifying scientific problems that should be considered when planning and executing scale-up experiments.

Table 1. Schematic on the three-step synthesis process for NKB/S, as well as quality control considerations for scale-up purposes

Synthesis Step	Precursors	Products	Quality Control Considerations
Mixing/Solvent Evaporation	PMF Ketjen Black (KB) Ethanol	PMF:KB	Homogeneity Evaporation Rate
Carbonization	PMF:KB	NKB	Degree of N-doping NKB Porosity
Sulfur Heat Treatment	NKB Sulfur	NKB/S	Sufficient wt.% S Consistent S Distribution in Pores Maximized yield of optimal particle size

2. Experimental Methods

2.1 Synthesis of NKB/S Material

All chemicals were used as received. Ketjen Black (KB, EC-600JD) was mixed with poly(melamine-co-formaldehyde) methylated (PMF, Sigma-Aldrich) with ethanol until all solvent

fully evaporated at room temperature. Upon fully evaporating, the PMF/KB integrated clusters were further dried for at least 12h under vacuum at 60°C. The clusters are then carbonized at 900°C under an argon atmosphere in a tube furnace for 10h and sieved with a 150µm mesh afterwards. The resulting NKB is then heat-treated with sulfur powder (Sigma-Aldrich) at 155°C for 12h. The ratio by mass of NKB to S in all batches is 1:4 to achieve 80 wt.% S content. The NKB/S powder is then grinded and sieved with 90 and 25µm meshes.

2.3 Material Characterization

X-ray diffraction (XRD) was conducted using a Bruker D8 Discover. Thermogravimetric analysis (TGA) was performed on a Mettler-Toledo TGA/DSC 3+ to determine the sulfur content of the composite. Nitrogen gas was used as the atmosphere while the test was conducted at a temperature range of 25-500°C with a heating rate of 10°C/min. A Hitachi TM3000 scanning electron microscope (SEM) was used for imaging the morphology of the material. Surface area of the NKB/S was quantified using an Anton Paar Nova 800 analyzer and applying the BET method.

2.4 Electrode Preparation

A binder solution was prepared with polyacrylic acid (PAA, M_w 1,250,000, Sigma-Aldrich) and lithium hydroxide (LiOH, anhydrous reagent grade >98%, Sigma-Aldrich) dispersed in water. NKB/S cathodes were subsequently prepared by mixing NKB/S from the 25-90µm range with multi-walled carbon nanotubes (MWCNT, MSE Supplies) and the binder solution at a solid content ratio of NKB/S:MWCNT:Binder = 80:16.9:3.1. The slurry was mixed thoroughly in a planetary centrifugal mixer (Thinky) with two zirconium mixing balls. The slurry was then coated on carbon coated aluminum foil (3µm thick carbon coating, 15µm thick foil, STOV Technology) with a doctor blade and minicoater (Hohnsen, Model MC20) at a thickness of 450µm. The cathode was

then dried in ambient conditions before being moved into a vacuum oven set to 60°C at half-vacuum pressure (-0.05MPa) for at least 12h.

2.5 Electrochemical Characterization

2032-type coin cells (MTI Corp.) were prepared inside an argon-filled glovebox using 250µm thick Li as the anode with a 16mm diameter and the NKB/S electrode with an area of 1.27cm^2 as the cathode. 25µm thick polyethylene (PE) was used as the separator in every coin cell tested. The electrolyte used for each coin cell contained 1M lithium bis(trifluoromethanesulfonyl)imide (LiTFSI, Gotion) in 1,3-dioxolane (DOL, Gotion) and 1,2-dimethoxyethane (DME, Gotion) (1:1, v/v) with 0.3M lithium nitrate salt ($LiNO_3$, Sigma Aldrich). Each coin cell was tested under both the flooded and lean condition, with an electrolyte-to-sulfur (E/S) ratio of 10µL/mg and 4µL/mg for flooded and lean, respectively.

The flooded condition coin cells were tested in a Neware MIHW-200-160CH battery tester. This tester held the cells at a constant temperature of 25°C. The lean condition cells were tested in a LANHE battery tester CT3001A at 30°C. The cells first rested for 6 hours, before undergoing two formation cycles at C/20 (1C = 1000mA/g) and subsequent cycling at C/10. All cycling occurred in a voltage window of 1.8-2.8V.

3. Results and Discussion

3.1 Materials Validation

Batches were validated to ensure the desired product was synthesized. Once the NKB/S material was synthesized, XRD was used to confirm the elemental composition of the composite. **Figure 2** compares the XRD spectra of NKB/S with elemental sulfur. It shows that the XRD spectra of a batch of NKB/S and that of sulfur are completely identical. XRD should show a spectrum that

reflects the composite's individual components, NKB and S. Owing to its amorphous structure, it would be expected that NKB would exhibit a spectrum with more broad peaks. Meanwhile, sulfur's most common natural allotrope, S_8, possesses crystallinity. This means that the XRD spectrum for sulfur should have sharp, distinct peaks. In a two-material composite that combines a crystalline component with an amorphous one, the spectra of the net composite should reflect that of the crystalline component after background reduction. And indeed, that is what is shown in the XRD spectra of the two materials. Once the chemical composition was confirmed, SEM was used to validate particle morphology. SEM images reveal particles with a rough surface, consistent with a porous particle that had been crushed during processing (**Figure 3**).

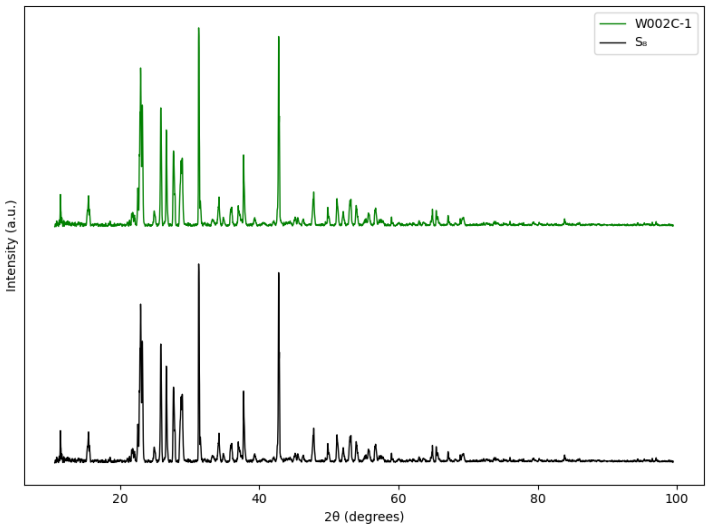

Figure 2. XRD spectra comparing an NKB/S batch with elemental S

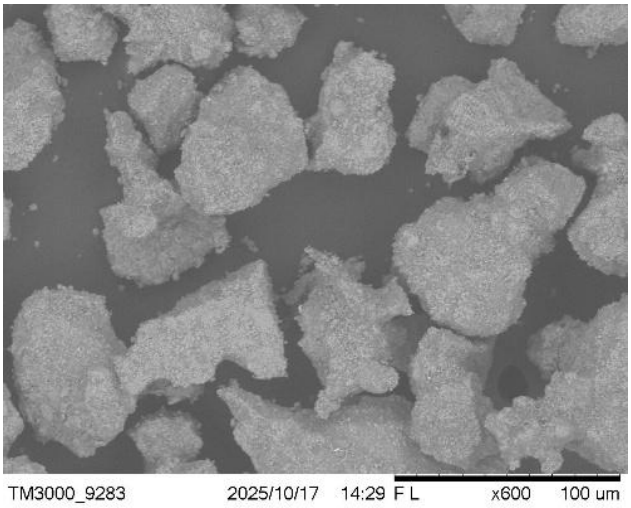

Figure 3. SEM image taken of NKB/S particles at the 25-90µm particle size range

Next, TGA was used to verify that the material had the designed 80 wt.% S present in the powder. In this method, the change in mass percent is proportional to the amount of sulfur sublimating out of the NKB host structure. However, in batch after batch, TGA analysis (**Figure 4**) shows a sulfur content that is consistently 2-4% higher than the target 80%. Human error was ruled out after performing the experiment multiple times and further validated by other collaborators.

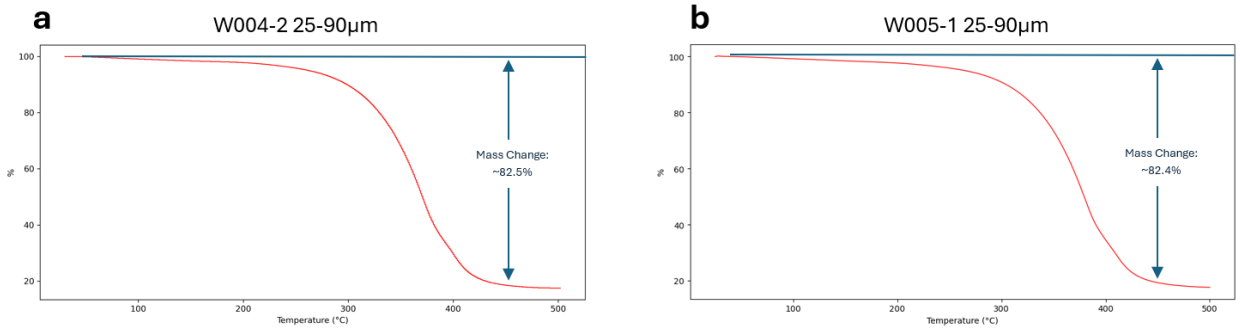

Figure 4. TGA of different batches of NKB/S synthesized at the desired 25-90µm particle size range

In the above case, TGA was only performed on the material that was sieved to the desired particle size range of 25-90µm. A hypothesis was then formed that the S wt.% could be inhomogeneous and dependent on the particle size range of the batches. To investigate this, further TGA analysis

was conducted on the various NKB/S batches, namely of the material <25µm (one such batch highlighted in **Figure 5**). The results show that, while the 25-90µm material had over 80 wt.% S, the <25µm material had under 80 wt.% S by an almost equal amount. In the case of one such batch, where the 25-90µm material had 82.5 wt.% S (**Figure 5a**), the <25µm material had 77.8 wt.% S (**Figure 5b**).

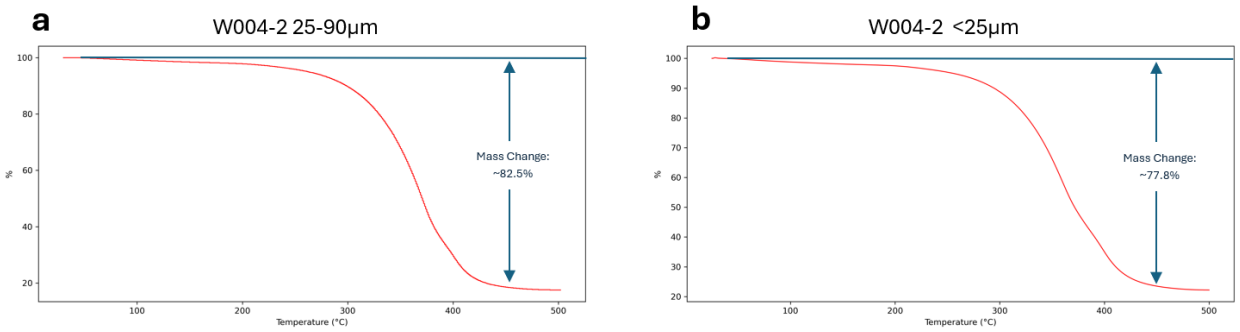

Figure 5. TGA of one batch of NKB/S at (a) the 25-90µm and (b) the <25µm particle size ranges

This inhomogeneous distribution is likely not caused by an inhomogeneous particle size mix; at multiple steps along the synthesis process, the NKB was tossed and mixed very well. Rather than that, a more likely explanation could be that either the pore structure and/or volume of the smaller NKB particles is not enough support a high sulfur content, while the same pore characteristics of larger particles may better facilitate it. During the synthesis of NKB, PMF was used essentially as a glue to incorporate KB nanoparticles together into NKB secondary particles by suspending them in the PMF/ethanol solution and evaporating away the solvent. Owing to the difficulty of suspending a highly porous carbon nanoparticle in solution without agglomeration, this process has many uncontrollable variables, and an inhomogeneous dispersion of KB into the PMF/ethanol solution could cause certain amounts of KB to be unincorporated. It can be therefore assumed, that a not-insignificant amount of the NKB under 25µm would be unincorporated KB. Smaller pore sizes in these smaller particles can lead to less sulfur infiltration during heat treatment, during

which time the melted sulfur may prefer to embed itself within the pores of the larger particles, provided there is enough space left over.

To begin investigating this, the average surface area of the material in the two NKB/S particle size ranges were determined using BET analysis. By obtaining the surface area, the particle's average pore characteristics can be inferred semi-quantitatively. Porous materials tend to have a high surface area, which gives a relative window into the pore volume of the particles. However, smaller particles such as porous nanoparticles, like KB, would also tend to have a high surface area. BET analysis, shown in **Figure 6**, reveals that the NKB/S in the smaller range have a much larger surface area than that of the larger range (19.726m^2/g compared to 11.244m^2/g in the larger range). The higher surface area could be suggesting that the <25µm NKB/S is more porous than the 25-90µm material, which would make sense if indeed many of those materials are unincorporated. If that is the case, potentially the pores in that material (again assumed to be unincorporated nanomaterial at that smaller particle size range) may be too small to support sulfur infiltration or preferred the N-doped incorporated material. Future studies could include the verification of pore structure using a technique such as x-ray computed tomography (CT) scans to better understand the reason why sulfur prefers the larger particle size range. Determining the degree of N-doping within the two particle size ranges could also be another possibility. Many of the quality control considerations highlighted in the later synthesis steps from **Table 1** could be highly influenced by those of the earlier steps, and the further verification could be used to validate this. It may provide also an opportunity to leverage some of these findings to create higher sulfur loading NKB/S in the future, potentially achieving a better performing Li-S battery.

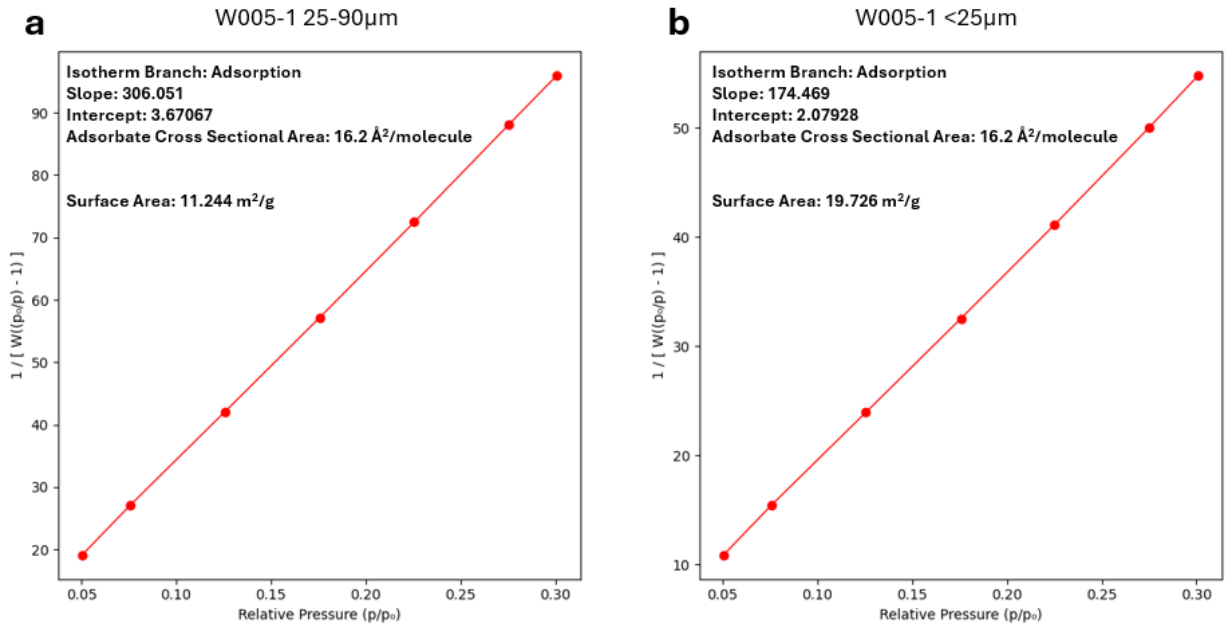

Figure 6. BET isotherms for (a) 25-90µm NKB/S and (b) <25µm NKB/S

3.2 Electrochemical Performance

Once the rationale for the different sulfur loading materials was identified, the material was fabricated into cathodes and tested electrochemically. Electrochemical validation of the NKB/S material was performed using coin cells. Practical conditions for Li-S cells require a high sulfur loading cathode and lean electrolyte. Flooded condition cells are less practical due to the added weight of the extra electrolyte causing the cell to have a lower energy density, but they offer a more reliable testing baseline in coin cells due to the large empty volume in the casing that necessitates the use of more electrolyte for reliable electrode wetting. Lean condition cells are generally more difficult to assemble consistently due to having less electrolyte available to wet the cathode. Compared to the flooded condition, it is expected that the cell can cycle at a higher specific capacity with better capacity retention after formation. This is due to the polysulfide shuttling effect; a flooded cell has more electrolyte in the system to act as the medium for the migration of polysulfides to the anode as well as their side reactions with the lithium metal, which

is not as pronounced with less electrolyte available in the lean condition. However, cells with this electrolyte condition will not cycle stably for as long as the flooded condition cells because the electrolyte will be spent more quickly with less of it available in the lean condition compared to the flooded. **Figure 7** shows results from both conditions tested. They show the characteristic double plateau voltage profile of Li-S cells, with the second plateau averaging around 2.1V. It can be seen from there that the first formation cycle can achieve above 1100mAh/g for both conditions, even exceeding 1200mAh/g in some cases. As expected, the flooded condition cells cycle stably for longer but experience a more severe initial capacity fade than the lean condition cells. Where the flooded cells could cycle around 900mAh/g for over 80 cycles, the lean condition cells could cycle closer to 1000mAh/g for around 50 before dropping off. The lean condition cells demonstrate a higher sulfur utilization rate under coin cell conditions.

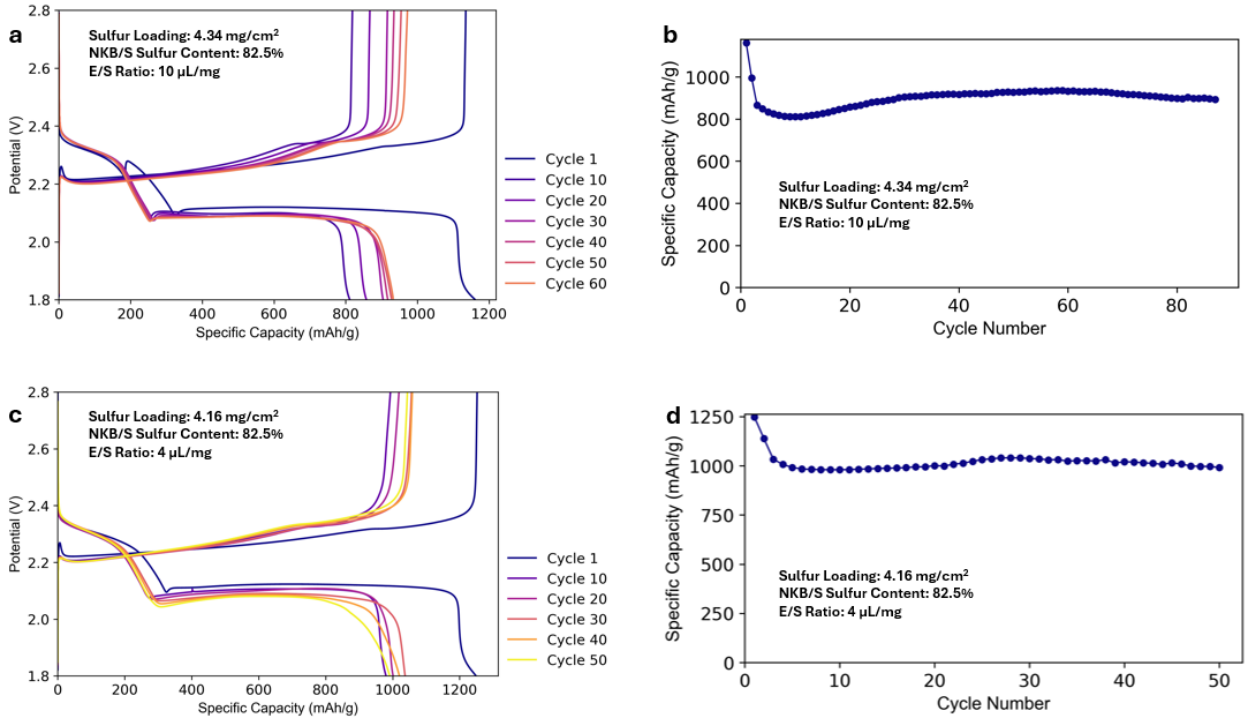

Figure 7. Voltage profiles of a (a) flooded condition NKB/S coin cell and a (c) lean condition cell and cycling performance (b) for the flooded cell and (d) for the lean cell

3.3 Implications

Further investigation is needed to accurately determine the exact cause of this unequal sulfur distribution, but there are still implications for scale-up research, regardless. To get down to the 80% target with the existing synthesis process, it could be as simple as sieving out the <25μm NKB before the S heat treatment process. Admittedly, this might be easier said than done considering the low tap densities of the NKB and KB could make sieving out smaller particle sizes very time-consuming, but it is an option. Getting rid of the smaller particles would allow the sulfur to more evenly distribute among the NKB within the ideal particle size range and achieve the target S content that way. Studies into the homogeneity of the NKB integration and carbonization could be another approach. If the way the KB is integrated into NKB can be better homogenized, that could play a role in helping to minimize the variance in S content across batches of NKB/S by reducing the amount of KB left unincorporated during the initial mixing and drying processes. Future work along these vectors will benefit the scaling up of this synthesis process and those similar to it, by providing considerations towards appropriate equipment and processing adjustments when increasing batch size.

4. Conclusion

In this study, lab-scale synthesis of the NKB/S cathode material for advanced Li-S batteries was conducted with a focus towards identifying scientific problems potentially associated with the scale-up and manufacturing. Over the course of this study, it was noticed that the sulfur content within the NKB/S composite was consistently higher than the target in batch after batch. During the investigation of this phenomenon, TGA analysis revealed that where there was extra mass percent sulfur in the usable particle size range, there was almost an equal percentage missing from the smaller, discarded particle sizes. This information, coupled with further study into the

underlying factors behind this, will better inform future efforts towards increasing the yield of usable active material while maintaining consistently good quality.

Acknowledgements

First and foremost, I would like to thank Professor Jie Xiao, my principal investigator. Whether it was by helping to set up the lab at the beginning, to working as her group's first lab manager, I had the chance to experience many things I never would have imagined possible prior. I will forever be grateful to her for taking a chance on me and for her subsequent generosity as I progressed with my research. I would also like to express my gratitude to my mentor, Cassidy Anderson, for guiding me throughout this project and putting up with my many questions. Balancing her own PhD research at PNNL while also dealing with me at UW could not have been easy for her, and I will always be thankful for her guidance and patience. Thank you to Dr. Yuchen Ji, for constantly reassuring me that my electrochemical results are in line with expectations as he tests Li-S cells for his own research and just being there to hear me out when I needed someone to talk to. Thank you to Kha Le for his assistance with electrode fabrication, as well as lean condition cell assembly and testing. Thank you to Dr. Dongping Lu at PNNL for sending precursors to me to help me get started on this project. And many thanks to Dr. Samantha Young, Scott Braswell, Joey Law and Babak Saidi at the UW Molecular Analysis Facility and the Washington Clean Energy Testbeds for training me on the relevant instrumentation and helping me conduct characterizations I didn't have time to train on.

To Shineui Hwang, Simon Danitz, Qixuan Jiang, Harvey Yang, Mirina Enderlin, Paola Manjarres, Patrick Zhuang and Kent Huang – the rest of Professor Xiao's Manufacturing Science & Engineering Lab – thank you for always keeping a warm, friendly and collaborative working environment both in and out of the lab. Between the laughs we shared, as well as the serious

conversations and scientific discussions, it's been a pleasure to share the lab with all of you. I would also like to extend my sincerest gratitude to Professor Jun Liu, Professor Jihui Yang, and their research groups for allowing me to use their lab spaces and equipment as necessary, as well as always being there to offer advice or just chat with me about various subjects. Special thanks to Professor Liu and his group (especially Dr. Mitchell Kaiser, Dr. Sicen Yu, Anthony Romero, Zhi Peng and Bella Wu), where my journey in research started, and whose recommendation led me to Professor Xiao's lab when I started my master's degree.

I would also like to extend my heartfelt gratitude towards my parents, Soo Bin Ng and Yu Hong Wu, for their constant and unwavering support over the years. They cultivated my interest in science and engineering and always did their best to provide help and/or advice to me when they felt I needed it. It is not an exaggeration to say that I would not be where I am today without them.

Finally, I would like to acknowledge that this research was supported by the Energy Efficiency and Renewable Energy, Office of Vehicle Technologies of the U.S. Department of Energy through the Advanced Battery Materials Research (BMR) Program (Battery500 Consortium and BMR under Contract No. DEAC0205CH11231).

References

[1] S. Feng, J. Liu, X. Zhang, L. Shi, C. Anderson, Y. Lin, M.-K. Song, J. Liu, J. Xiao, D. Lu, *Nano Energy* 2022, 103, 107794.

[2] Z. W. Seh, Y. Sun, Q. Zhang, Y. Cui, *Chem. Soc. Rev.* **2016**, *45*, 5605.

[3] S. S. Zhang, *Journal of Power Sources* **2013**, *231*, 153.

[4] Y. V. Mikhaylik, I. Kovalev, R. Schock, K. Kumaresan, J. Xu, J. Affinito, *ECS Trans.* **2010**, *25*, 23.

[5] J. Ke, Z. Wang, H. Zhu, M. Chen, R. Song, Q. Ji, D. Liu, S. Lan, *Commun Mater* **2025**, *6*, 237.

[6] Y.-X. Yin, S. Xin, Y.-G. Guo, L.-J. Wan, *Angewandte Chemie International Edition* **2013**, *52*, 13186.

[7] T.-H. Tsai, Y.-S. Su, *RSC Appl. Interfaces* **2025**, *2*, 1105.

[8] A. Eftekhari, D.-W. Kim, *J. Mater. Chem. A* **2017**, *5*, 17734.

[9] F. Wu, J. Chen, R. Chen, S. Wu, L. Li, S. Chen, T. Zhao, *J. Phys. Chem. C* **2011**, *115*, 6057.

[10] J. Wang, J. Chen, K. Konstantinov, L. Zhao, S. H. Ng, G. X. Wang, Z. P. Guo, H. K. Liu, *Electrochimica Acta* **2006**, *51*, 4634.

[11] L. Xiao, Y. Cao, J. Xiao, B. Schwenzer, M. H. Engelhard, L. V. Saraf, Z. Nie, G. J. Exarhos, J. Liu, *Advanced Materials* **2012**, *24*, 1176.

[12] J. Song, M. L. Gordin, T. Xu, S. Chen, Z. Yu, H. Sohn, J. Lu, Y. Ren, Y. Duan, D. Wang, *Angewandte Chemie International Edition* **2015**, *54*, 4325.